MATHEMATICAL BIOSCIENCES
AND ENGINEERING
Volume **6**, Number **1**, January **2009**

doi:10.3934/mbe.2009.6.27

pp. **27–40**

A LUMPED MODEL FOR BLOOD FLOW AND PRESSURE IN THE SYSTEMIC ARTERIES BASED ON AN APPROXIMATE VELOCITY PROFILE FUNCTION

Wouter Huberts and E. Marielle H. Bosboom

Department of Biomedical Engineering
Eindhoven University of Technology
University Hospital Maastricht
PO Box 5800, Maastricht, The Netherlands

Frans N. van de Vosse

Department of Biomedical Engineering
Eindhoven University of Technology
PO Box 513, Eindhoven, The Netherlands

(Communicated by Mette Olufsen)

Abstract. Previously, by assuming a viscous dominated flow in the boundary layer and an inertia dominated flow in the vessel core, a velocity profile function for a 1D-wave propagation model was derived. Because the time dependent shape of the velocity profile in this boundary layer model depends on the size of the inviscid core and the boundary layer, and thus on the Womersley number, it differs along the arterial tree. In this study we evaluated a lumped model for a vessel segment in which the element configuration is based on physical phenomena described by the boundary layer model and for which all parameters have a physically based quantitative value dependent on the Womersley number. The proposed electrical analog consists of a Womersley number dependent resistor and an inductor arranged in parallel, representing the flow impedance in respectively the vessel core and the boundary layer, in series with a second resistor. After incorporating a capacitor representing the vessel compliance in this rigid tube model, the element configuration resembles the configuration of the four-element windkessel model. For arbitrary Womersley numbers the relative impedance of Womersley theory is approximated with high accuracy. In the limits for small and large Womersley numbers the relative impedances of the proposed lumped model correspond exactly to Womersley theory.

1. **Introduction.** Windkessel [3, 14, 15, 17] as well as lumped parameter models [4, 5, 6, 7, 11, 12, 13, 16] are used to simulate pressure and blood flow in the arterial system. The first windkessel model was introduced by Frank et al. [3]. This model consists of a capacitor representing the aortic compliance and a constant resistor representing the peripheral resistance. Westerhof et al. [17] extended this model with an extra resistor, which is thought to be the aortic characteristic impedance. As a result, a better representation of the medium- to high-frequency behavior of the systemic input impedance is obtained. Stergiopulos et al. [15] concluded that

2000 *Mathematics Subject Classification.* 76Z05, 92C35.

Key words and phrases. lumped parameter approach, approximate velocity profile function, windkessel model, arterial modeling, electrical analog.

The first author is supported by the profileringsfonds of the University Hospital Maastricht.

the four-element Windkessel model with an inertial term in parallel with the characteristic impedance, is even superior to the three-element Windkessel model in describing the behavior of the entire systemic tree or as a model for parameter estimation of vascular properties. Stergiopulos et al. concluded that the inertial term represents the total inertia of the blood. In addition, they stated that for the aorta the configuration of an inertial term in parallel with a characteristic impedance seems correct because for high frequencies the aorta behaves like a reflectionless tube and for low frequencies the local properties of the aorta (i.e., the characteristic impedance) are negligible. However, a quantitative physical origin for a parallel configuration was not given.

Windkessel models fail to explain the phenomena of pulse wave propagation throughout the arterial tree, as the inherent property of the windkessel model assumes an infinite wave velocity. To study the wave phenomenon, therefore, arterial tree models based on transmission line theory have been developed [9, 16]. For these models the vascular system is divided (lumped) into segments that represent the local blood (density ρ, kinematic viscosity ν) and vessel wall (radius a, compliance C_v) properties. All segments are connected based on the anatomical configuration to obtain a transmission line. These lumped parameter models include the multi-branched configuration of the arterial system and a description of the distributed nature of arterial properties. In Noordergraaf's model [9] a passive electrical analog was chosen, which was based on a comparison between equations describing propagation along a transmission line (the two telegraph equations) on the one hand and a simplified equation of motion of the blood and the equation of continuity for fluid flow in a short arterial segment on the other hand. The lumped segments consisted of an inductor L in series with a resistor R that represent respectively the blood inertia and the viscous blood resistance (Fig. 1). In addition, the compliance C of the vessel wall was modeled with a capacitor. In large arteries (Womersley number $\alpha = a\sqrt{\frac{\omega}{\nu}} \gg 1$), like the aorta, the wave phenomena are inertia dominated and a good approximation of the parameters of the lumped model (values for R and L) can be derived from the vessel geometry and mechanical properties using a flat velocity profile. In small vessels ($\alpha \ll 1$), i.e. arteries with a diameter smaller than 2 mm, viscous forces are dominant and approximate values for R and L can be derived using a quasi-static Poiseuille profile. In Noordergraaf's model a flat velocity profile is assumed in the calculation for the inertial term whereas a parabolic velocity profile is assumed for the viscous term, so the two limiting cases were combined in each of the single vessels independent of the size and frequency of the pressure and flow pulsations. Because of the pulsatile nature of the blood flow a phase difference will be present between the velocity in the core of the vessel and the velocity in the boundary layer close to the vessel wall. However, this will lead to frequency dependent values for the inductor L and resistor R. To take the balance between viscous and inertial forces into account, Jager et al. derived an extended electrical network [6], that consisted of several frequency independent inductors and resistors for every segment (Fig. 1). At higher Womersley numbers, a higher number of extra resistors and inductors were needed to accurately describe the longitudinal impedance [6]. Given the radii of the arteries and the harmonic that contains most wave energy, it is possible to derive an electrical transmission line of the total arterial tree that incorporates the balance between inertia and viscous forces. Such a model was made by Westerhof et al. [16], however, the network configuration is complex and totally based on a mathematical derivation in which

the physical origin of the pressure and flow waves is not apparent.

Olufsen et al. [10] derived lumped models starting with the one-dimensional axisymmetric Navier-Stokes equation for time-dependent blood flow in rigid tubes and by applying Laplace transformation and inversion via residue theory. For tubes with a radius between 5 and 15 mm (i.e. Womersley numbers between approximately 5 and 15) Olufsen et al. found a lumped model which has the same configuration as the four-element windkessel model. This model configuration is less complex than Jager's network. However, the values of the resistor and inductor did not depend on the Womersley number, but were assumed to be constant for a range of radii. In this study, we aim to derive a lumped model for a vessel in which the element configuration is based on physical phenomena and for which all parameters have a physically based quantitative value dependent on the Womersley number. In the limiting cases for small and large Womersley numbers, the impedance of the derived lumped model should correspond to Womersley theory.

We based this study on a wave propagation model with a time and frequency dependent approximate velocity profile function derived by Bessems et al. [2]. They developed a one-dimensional model of blood flow in arteries without a priori assuming a shape for the velocity profile. The resulting approximate velocity profile consists of an inertia dominated flow in the core of the vessel and a viscous dominated flow near the vessel wall. The size of the inviscid core and the boundary layer depend on the Womersley number. Therefore in this model the various velocity profile shapes along the arterial tree differ and form a good approximation of the velocity profiles obtained from Womersley theory [18] with respect to the nonlinear term $\int v_z^2 d\Omega$ and the friction term $\eta \int \frac{\partial v_z}{\partial r} d\Gamma$ [2].

To capture this in an electrical analog, intuitively, an inductor in parallel with a resistor is expected, representing the flow impedance in respectively the core of the vessel and near the vessel wall. Because for steady flow the total vessel impedance in the electrical analog should converge to a Poiseuille resistance, a Poiseuille resistor is added in series with the parallel arrangement of the inductor and resistor. In this paper, in Section 2, the approximate velocity profile function given by Bessems et al. is briefly described. In addition, mathematical expressions for the parameters in the proposed lumped model are derived. Thereafter, in Section 3, the relative impedance of the proposed lumped model normalized to the Poiseuille resistance is compared with the relative impedance derived from the approximate velocity profile function to motivate our choices. Next, the relative impedance is compared with Womersley theory to show the difference between Womersley theory and our model. In addition, the limiting cases for the relative impedances of the proposed lumped model and Womersley theory are compared. This is done for large ($\alpha \gg 1$) and small ($\alpha \ll 1$) Womersley numbers, representing respectively a flat and a parabolic velocity profile. Furthermore, simplified models are derived in case of Womersley numbers $\alpha \leq \sqrt{2}$ and $\alpha > \sqrt{2}$. These $\sqrt{2}$-limits stem from the derivation of the approximate velocity profile. Finally, the proposed lumped model is discussed in Section 4 and our findings are compared with literature.

2. **Methods: Derivation of the lumped model.**

The lumped model proposed in this article is based on the wave propagation model with an approximate velocity profile function that was derived by Bessems et al. [2] and is further referred to as boundary layer model. In the first subsection the approximate velocity profile function will be described shortly. For a detailed derivation we refer to Bessems et

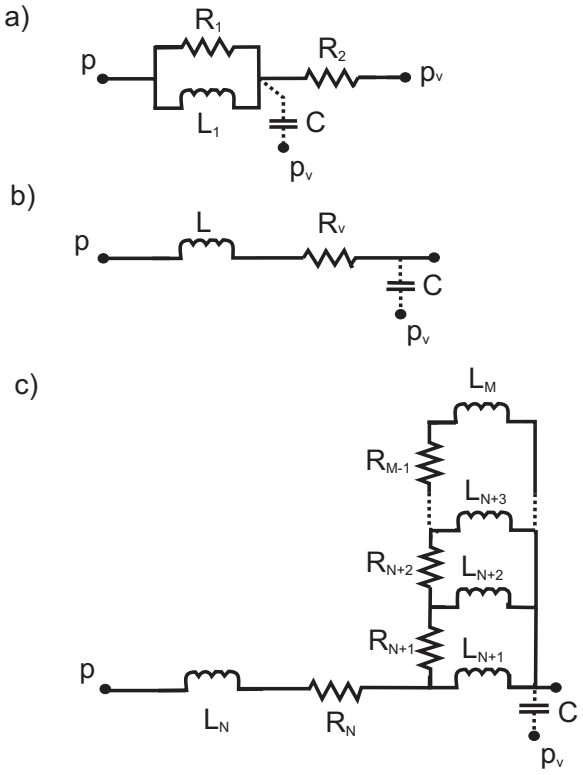

FIGURE 1. The electrical analog of the longitudinal impedance of a) the proposed electrical analog based on the boundary layer model, b) Noordergraaf's model and c) Jager's model. The capacitor C can be added to obtain a compliant tube model.

al. [2]. An experimental validation of the model can be found in Bessems et al. [1]. The derivation of our electrical analog is described in the second subsection.

2.1. **The approximate velocity profile function.** To derive the approximate velocity profile function, Bessems et al. [2] considered the Navier-Stokes equation for fully developed flow in straight tubes driven by a given pressure gradient:

$$\rho\frac{\partial v_z}{\partial t} = -\frac{\partial p}{\partial z} + \eta\frac{1}{r}\frac{\partial}{\partial r}(r\frac{\partial v_z}{\partial r}) \tag{1}$$

in which v_z is the axial velocity, $\frac{\partial p}{\partial z}$ the pressure gradient, η the dynamic viscosity and r the radial coordinate.
In the boundary layer close to the vessel wall the viscous forces are dominant whereas in the center of the vessel the inertial forces are dominant. Between the viscous boundary layer and the vessel core there is then a transition layer in which a balance between viscous and inertial forces exists, as described by (1). Bessems et al. [2] assume the transition layer to become infinitely small. In addition, it is assumed that there is a balance between the inertial forces and the viscous forces at the transition from the boundary layer to the central core and that at the transition in the axial direction the velocity in the boundary layer equals the velocity in the

central core. Under these assumptions it can be derived that the relation between the size of the central core and the Womersley number α can be given by:

$$\frac{a_c}{a} = \max[0, 1 - \frac{\sqrt{2}}{\alpha}] \tag{2}$$

in which $a_c(\alpha)$ is the Womersley number dependent radius of the central core and a is the vessel radius. The velocity profile function given by Bessems et al. is related to $\zeta_c = (\frac{a_c}{a})^2$ according to the following equation:

$$v_z = -\frac{\ln \hat{\zeta}}{1-\zeta_c}\frac{q}{A} - \frac{a^2}{4\eta}[1 - \hat{\zeta} + \frac{1}{2}(\zeta_c + 1)\ln \hat{\zeta}] - \frac{\partial p}{\partial z} \tag{3}$$

in which q is the flow, A the cross-sectional area, and $\hat{\zeta} = \max[(\frac{r}{a})^2, \zeta_c]$. The shapes of the velocity profiles along the arterial tree computed with this boundary layer model are a good approximation of the velocity profiles obtained from Womersley theory with respect to the nonlinear term $\int v_z^2 d\Omega$ and the friction term $\eta \int \frac{\partial v_z}{\partial r} d\Gamma$ [2]. The advantage of the boundary layer model is that it can be applied in the time domain.

2.2. **Derivation of the lumped model.** To derive a lumped model we use the same assumptions as Bessems et al. in the derivation of its approximate velocity profile function. Intuitively, the lumped model consists then of a parallel arrangement of a resistor per segment length R_1 and an inertance per segment length L_1 that represent respectively the viscous resistance in the boundary layer and the inertia dominated impedance in the central core. To let the electrical model converge to a Poiseuille resistance for steady flow a second resistor R_2 is introduced in series with the parallelly arranged R_1 and L_1 (Fig. 1). The derivation is restricted to rigid tubes, but can easily be extended with a capacitor to model the storage capacity of the vessel without changing the derived model parameters.

In this subsection the derivation of mathematical expressions for the resistors R_1 and for the inertance L_1 from the boundary layer model proposed by Bessems et al. [2] is described. A mathematical expression for the resistor R_2 follows directly from the definition of a Poiseuille resistance. The other two parameters are derived by comparing the longitudinal impedance of the proposed electrical analog with the longitudinal impedance in the boundary layer model. The longitudinal impedances are complex numbers and because the longitudinal impedances of both models should be the same, the real and imaginary parts are compared separately. In this way two equations with two unknowns (R_1 and L_1) are obtained. From those two equations, the mathematical expressions for R_1 and L_1 are derived.
In Bessems' boundary layer model, by neglecting the external forces —the nonlinear term and the diffusion term, the 1D-momentum equation for flow through a rigid vessel is given by [2]:

$$-\frac{\partial p}{\partial z} = [\frac{c_q}{2-c_p}]R_v q + [\frac{1}{2-c_p}]L\frac{\partial q}{\partial t} \tag{4}$$

in which p is the pressure, z is the longitudinal direction, R_v is the Poiseuille resistance per segment length ($\frac{8\eta}{\pi a^4}$), and L is the inertia per segment length ($\frac{\rho}{\pi a^2}$). The functions c_p and c_q are dependent on the squared radius of the vessel core ζ_c

and thus on the Womersley number α according to [2]:

$$c_p = 1 + \frac{1}{2}(1-\zeta_c) \qquad \text{and} \qquad c_q = \frac{1}{2}(1-\zeta_c)^{-1}. \tag{5}$$

For Womersley numbers smaller than $\alpha \leq \sqrt{2}$ the central core disappears, see (2), resulting in Poiseuille flow. By using (5), c_p and c_q for $\alpha \leq \sqrt{2}$ are given by:

$$c_p = 3/2, \qquad c_q = 1/2. \tag{6}$$

For large Womersley numbers ($\alpha > \sqrt{2}$) c_p and c_q depend on the core radius. After substitution of (2) in (5) c_p and c_q are given by [2]:

$$c_p = 1 + \frac{\sqrt{2}}{\alpha}(1 - \frac{\sqrt{2}}{2\alpha}), \qquad c_q = \frac{\alpha}{4\sqrt{2}}(1 - \frac{\sqrt{2}}{2\alpha})^{-1}. \tag{7}$$

By introducing the harmonics

$$\frac{\partial p}{\partial z} = \frac{\partial \hat{p}}{\partial z} e^{j\omega t} \tag{8}$$

and

$$q = \hat{q} e^{j\omega t} \tag{9}$$

the longitudinal impedance of the rigid vessel, Z_l^b, can be derived to be:

$$Z_l^b = \frac{-\frac{\partial \hat{p}}{\partial z}}{\hat{q}} = [\frac{c_q - (2-c_p)}{2-c_p}]R_v + j\omega L[\frac{1}{2-c_p}] + R_v. \tag{10}$$

The longitudinal impedance for the electrical analog Z_l^e in Figure 1 is given by:

$$Z_l^e = j\frac{\omega R_1^2 L_1}{R_1^2 + \omega^2 L_1^2} + \frac{\omega^2 L_1^2 R_1}{R_1^2 + \omega^2 L_1^2} + R_2. \tag{11}$$

Because the total vessel impedance should converge to a Poiseuille resistance for steady flow in the electrical analog, R_2 equals a Poiseuille resistance. By comparing the real and imaginary parts of (10) and (11) the mathematical expressions derived for the model parameters per segment length are derived:

$$R_1 = f(\alpha)R_v \tag{12}$$

$$L_1 = g(\alpha)L \tag{13}$$

$$R_2 = R_v \tag{14}$$

with

$$f(\alpha) = [\frac{c_q - (2-c_p)}{2-c_p} + \frac{\alpha^4}{64(c_q - (2-c_p))(2-c_p)}], \tag{15}$$

and

$$g(\alpha) = [64\frac{(c_q - (2-c_p))^2}{(2-c_p)\alpha^4} + \frac{1}{2-c_p}]. \tag{16}$$

As can be seen in Figure 2, the function $f(\alpha)$ is a smooth curve that goes to infinity for both large and small Womersley numbers. Function $g(\alpha)$ monotonically decreases to 1 for $\alpha > \sqrt{2}$ and has a constant value 2 for $\alpha \leq \sqrt{2}$. The limiting cases are discussed in the next section where the derived lumped model is compared with Womersley theory and the boundary layer model described by Bessems [2].

3. **Results: Comparison between the lumped model, boundary layer model and Womersley theory.**

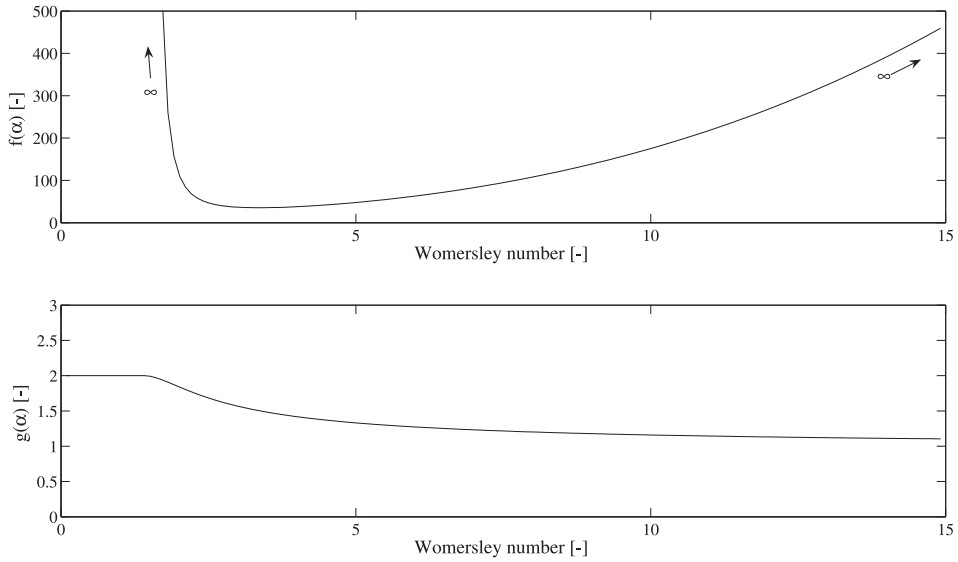

FIGURE 2. The functions $f(\alpha)$ (top) and $g(\alpha)$ (bottom) as a function of the Womersley number. The function $f(\alpha)$ converges to infinity for both $\alpha \to \infty$ and $\alpha \to 0$.

3.1. **Relative impedance.** In this section, the relative impedance of the proposed electrical analog, the Womersley theory and Bessems' boundary layer model are compared. The relative impedance I is defined as the longitudinal impedance (Z_l) normalized with the Poiseuille resistance R_v. From the definition of the Womersley number it can be derived that:

$$\frac{\omega L}{R_v} = \frac{\alpha^2}{8}. \tag{17}$$

After substitution of (12), (13), (14) and (17) in (11) the relative impedance for the electrical analog is given by:

$$I^e = \frac{Z_l^e}{R_v} = \frac{j\frac{\alpha^2}{8}g(\alpha)}{1 + j\frac{\alpha^2}{8}\frac{g(\alpha)}{f(\alpha)}} + 1. \tag{18}$$

The relative impedance for the boundary layer model is:

$$I^b = \frac{Z_l^b}{R_v} = \frac{c_q}{2 - c_p} + j\frac{\alpha^2}{8}\frac{1}{2 - c_p}, \tag{19}$$

while the relative impedance for Womersley reads [18]:

$$I^w = \frac{Z_l^w}{R_v} = j\frac{\alpha^2}{8}\frac{1}{1 - F_{10}(\alpha)} \tag{20}$$

in which F_{10} is the Womersley function.
As a reference, the relative impedance is also given for an electrical analog consisting of an inductor and resistor in series (Fig. 1) as introduced by Noordergraaf [9]:

$$I^n = \frac{Z_l^n}{R_v} = j\frac{\alpha^2}{8} + 1. \tag{21}$$

In Figure 3 the relative impedance of the lumped model is compared with both boundary layer model and Womersley theory. As expected, a perfect match is found for the impedances for the lumped model and the boundary layer model. For both models differences with Womersley theory are very small, i.e., much smaller than for Noordergraaf's model, and only visible in the phase angle for Womersley numbers between 1 and 6.

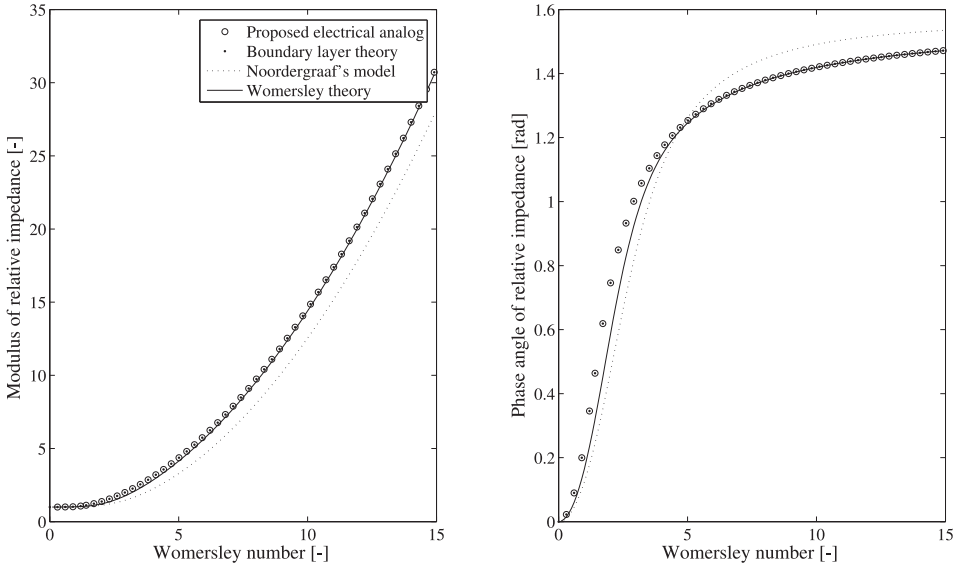

FIGURE 3. The modulus (left) and phase angle (right) of the relative impedance from the lumped model (circles), the boundary layer model (points), Noordergraaf's model (dotted line), and Womersley theory (solid line) as a function of the Womersley number.

3.2. **Limiting cases.** To investigate if the limiting behavior of the relative impedances of the proposed electrical analog and Womersley theory are consistent, the limiting cases for a parabolic ($\alpha \ll 1$) and a flat ($\alpha \gg 1$) velocity profile are examined.

The relative impedance for large Womersley numbers ($\alpha \gg 1$)
For $\alpha > \sqrt{2}$ in the boundary layer model c_q and c_p are defined by (7). The relative impedance of our proposed electrical analog yields after substitution of (7), (15) and (16) in (18):

$$I^e = \frac{\alpha^4}{4\sqrt{2}\alpha^3 - 12\alpha^2 + 8\sqrt{2}\alpha - 4} + j\frac{\alpha^5}{8\alpha^3 - 8\sqrt{2}\alpha^2 + 8\alpha} \tag{22}$$

which can be approximated by

$$I^e \approx \frac{\alpha}{4\sqrt{2}} + j\frac{\alpha^2}{8} \qquad \text{for } \alpha \gg 1. \tag{23}$$

The relative impedance based on Womersley theory is given by (see appendix)

$$I^w \approx \frac{\alpha}{4\sqrt{2}} + j\frac{\alpha^2}{8}, \qquad \text{for } \alpha \gg 1. \tag{24}$$

The approximate longitudinal impedances for the electrical analog and for Womersley theory can per definition be obtained by multiplying respectively (23) and (24) with the Poiseuille resistance R_v. By substituting (17) in (23) and (24), the longitudinal impedances for $\alpha \gg 1$ for both the electrical analog and Womersley theory are after neglecting the real part represented by the longitudinal impedance of an inertance, i.e., a flat velocity profile results.

The relative impedance for small Womersley numbers ($\alpha \ll 1$)
For $\alpha \leq \sqrt{2}$ in the boundary layer model c_q and c_p are defined as constants and respectively $\frac{1}{2}$ and $\frac{3}{2}$. For $g(\alpha)$ this gives:

$$g(\alpha \leq \sqrt{2}) = 2. \tag{25}$$

As the denominator of $f(\alpha)$ is 0 for all Womersley numbers smaller than $\sqrt{2}$, the reciprocal of $f(\alpha)$ for $\alpha \leq \sqrt{2}$ is determined by

$$\frac{1}{f(\alpha)} = \frac{(c_q(\alpha) - (2 - c_p(\alpha)))(2 - c_p(\alpha))64}{64(c_q(\alpha) - (2 - c_p(\alpha)))^2 + \alpha^4} = \frac{0}{\alpha^4}. \tag{26}$$

After substitution of the equations (25) and (26) in (18), the relative impedance on the domain $\alpha \in (0, \sqrt{2}]$ is given by

$$I^e = 1 + j\frac{\alpha^2}{4}. \tag{27}$$

For $\alpha \ll 3$ the relative impedance based on Womersley theory is (see appendix)

$$I^w \approx 1 + j\frac{\alpha^2}{4}. \tag{28}$$

The approximate longitudinal impedances for both the electrical analog and Womersley theory can per definition be obtained by multiplying respectively (27) and (28) with the Poiseuille resistance R_v. By using (27) and (28), the longitudinal impedances for $\alpha \ll 1$ for both the electrical analog and Womersley theory are after neglecting the imaginary part represented by the longitudinal impedance of a Poiseuille resistor, i.e. a parabolic velocity profile results.

3.3. **Simplified models.** The resistor R_1 and the inertia L_1 in Figure 1 are only dependent on the Womersley number as is derived in equation (12) and (13). It is thus possible to derive simplified lumped models that can be solved in the time-domain by assuming a characteristic Womersley number. In this section we derive simplified lumped models for Womersley numbers smaller than $\sqrt{2}$, as in this case only Poiseuille flow remains in the boundary layer model, and for Womersley numbers larger than $\sqrt{2}$).

Womersley number $\alpha \leq \sqrt{2}$
As was shown in Section 3.2 the function $f(\alpha)$ for Womersley numbers smaller than $\sqrt{2}$ is infinitely large and thus flow through resistor R_1 is blocked. A simplified model then consists of an inertance of $2L$ in series with a Poiseuille resistance. If the Womersley number decreases to zero, the relative impedance in (27) decreases to 1. $\alpha \leq \sqrt{2}$ the modulus of the relative impedance in (27) differs less than 12%

from 1 and because we consider this as not significant, the longitudinal impedance Z_l^e can be approximated by R_v. The simplified electrical analog then consists of only a resistor R_v.

Womersley number $\alpha > \sqrt{2}$

Functions $f(\alpha)$ and $g(\alpha)$ are plotted in Figure 2 for Womersley numbers between $0 < \alpha \leq 15$. It can be seen from this figure and equation (12) that the resistance R_1 of the boundary layer increases with increasing Womersley number. This can be explained from the fact that the boundary layer becomes thinner with increasing Womersley number, whereas the central core thickens. The latter can be seen in Figure 2 from a decreasing $g(\alpha)$. To come to simplified models for $\alpha > \sqrt{2}$ the ratio between the impedances of R_1 and L_1 needs to be studied more thoroughly. By using (17) this ratio is given by:

$$\frac{Z_{R_1}}{Z_{L_1}} = \frac{R_v f(\alpha)}{j\omega L g(\alpha))} = \frac{8 f(\alpha)}{j\alpha^2 g(\alpha)}. \tag{29}$$

The modulus and argument of equation (29) are given in Figure 4. The phase difference is $\frac{\pi}{2}$ radians which is expected as the impedance Z_{L_1} is purely imaginary while the impedance of the resistor Z_{R_1} is real. The modulus remains larger than one for all Womersley numbers and Z_{R_1} is at least eleven times higher than Z_{L_1}. Based on this observation the resistor R_1 can be omitted from the proposed electrical analog because the vast majority of the flow will go through the inertance. A simplified electrical analog with an inertance in series with a Poiseuille resistance is then obtained.

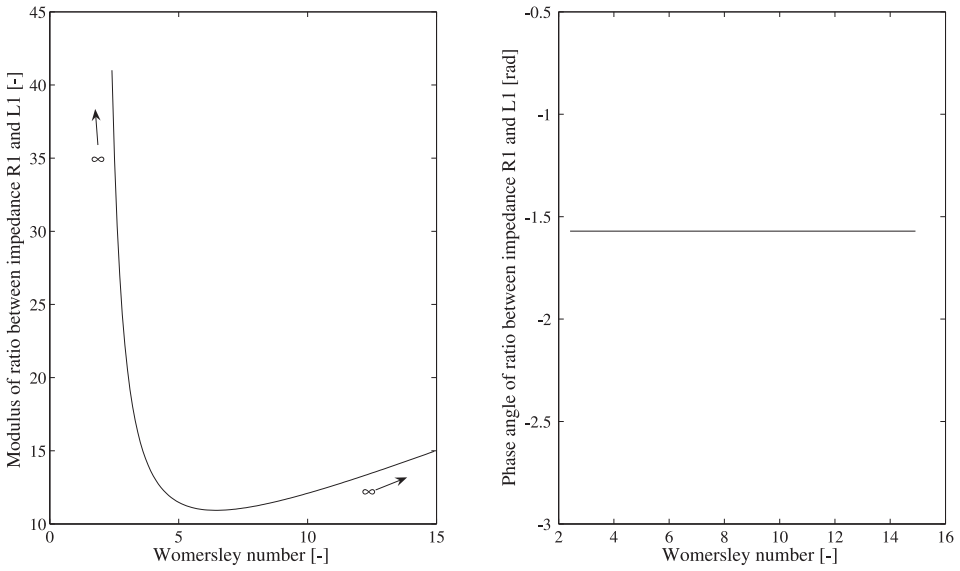

FIGURE 4. The modulus (left) and phase angle (right) of the impedance ratio $\frac{Z_{R_1}}{Z_{L_1}}$ as a function of the Womersley number.

4. **Discussion.** In this study we aimed to derive a simple lumped model for a vessel segment in which the element configuration is based on physical phenomena described by a boundary layer model and for which all parameters have a physically based quantitative value dependent on the Womersley number.

An electrical analog was derived based on the boundary layer model that was derived by Bessems et al. [2]. They assumed viscous dominated flow in the boundary layer and inertia dominated flow in the vessel core. Therefore, after neglecting the external forces, the nonlinear term and the diffusion term in the 1D-momentum equation, mathematical expressions were derived for an electrical analog that consists of a parallel arrangement of a resistor and an inertance per segment length that represent respectively the viscous resistance in the boundary layer and the inertia dominated impedance in the central core. In series with those parallelly arranged elements a Poiseuille resistance was introduced so that for steady ($\alpha = 0$) viscous flow a Poiseuille resistance is obtained in the electrical analog. The inertia of the core and the resistance of the boundary layer are fully described by fluid density, fluid viscosity, vessel diameter, and Womersley number. The difference between the relative impedances of the proposed lumped model and Womersley theory was very small, i.e. much smaller than for Noordergraaf's model, and only visible in the phase angle for Womersley numbers between 1 and 6. For both large ($\alpha \gg 1$) and small ($\alpha \ll 1$) Womersley numbers, the relative impedance of the proposed model was consistent with Womersley theory.
The model configuration proposed in this study was also found by Olufsen et al. [10] for vessels with a radius between 5 and 15 mm. The parameters for their model were $L_1 \approx \frac{4}{3}L$, $R_1 \approx 4\frac{1}{4}R_v$ and $R_2 = R_v$. In our analysis we find a L_1 that varies between L and $2L$ depending on the Womersley number; for $\alpha = 5$ holds $L_1 = \frac{4}{3}L$. The resistor R_1 in our analysis is significantly higher (at least a factor 8 for $\alpha = 3$) than in the lumped model proposed by Olufsen et al. for all Womersley numbers. A high R_1 is in accordance with the findings of Westerhof et al. as a network of segments consisting of a resistor and inductor in series suffices to model the whole vascular bed [16].

If a capacitor is added to our proposed electrical analog (Fig. 1), the model consists of the same elements as the four-element windkessel model proposed by Stergiopulos et al. [15]. It thus provides some justification for positioning the additional inertial term in the four-element windkessel model in parallel to the first resistor. Our lumped model suggests that the inertial term represents the inertia-dominated flow in the central core of the vessels, which is supported by Stergiopulos' conclusion that the inductor in the windkessel model represents the total blood inertance of the system. However, the four-element windkessel model is used to represent the cardiovascular system as a whole, whereas the lumped model in this study is derived by considering flow in a single segment.

By assuming the characteristic frequency (i.e., the harmonic that contains most of the wave energy) and using the mathematical expressions derived in this study, it is possible to derive expressions for segments that can be used to model a rigid tube model in the time-domain. A compliant tube model can be obtained after introducing a capacitor to each of the vessel segments (Fig. 1). By adding the compliant tube models together in series, it would also be possible to develop a transmission line model of the total arterial tree. However, only a slight improvement of the total vascular impedance is expected compared to a network built from segments only

containing a resistor and inductor in series and a capacitor. This because a comparison of the impedance moduli Z_{L_1} and Z_{R_1} showed that Z_{R_1} is at least one order higher and thus can be omitted from the lumped model. This is supported by the findings of Westerhof et al. [16], who incorporated the extra network introduced by Jager [6] in his transmission line model [16], and found that the extra network only slightly improved the input impedance of the systemic arterial tree compared to a network built from segments only containing a resistor and inductor in series and a capacitor. Although the improvements of the input impedance of the transmission line that consists of tube segments proposed in this article are expected to be small, all the electrical elements in such a line will be related to physical phenomena.

5. **Conclusion.** We were able to derive a simple lumped model for which all parameters have a physically based quantitative value dependent on the Womersley number and in which the element configuration is based on physical phenomena described by a wave propagation model with an approximate velocity profile function. After incorporating a capacitor representing the vessel compliance in this rigid tube model, the element configuration resembles the configuration of the four-element windkessel model. For arbitrary Womersley numbers the relative impedance of Womersley theory is approximated with high accuracy. In the limits for small and large Womersley numbers the relative impedances of the proposed lumped model correspond exactly to Womersley theory.

Appendix: The relative impedance for Womersley theory for small and large Womersley parameters. The relative impedance I is defined as the longitudinal impedance (Z_l) normalized with the Poiseuille resistance R_v. From the definition of the Womersley number it can be derived that:

$$\frac{\omega L}{R_v} = \frac{\alpha^2}{8}. \tag{30}$$

After substitution of (30) the relative impedance for Womersley reads [18]:

$$I^w = \frac{Z_l^w}{R_v} = j\frac{\alpha^2}{8}\frac{1}{1 - F_{10}(\alpha)} \tag{31}$$

in which F_{10} is the Womersley function.
The Womersley function F_{10} is defined as [18]:

$$F_{10} = \frac{2J_1(j^{3/2}\alpha)}{j^{3/2}\alpha J_0(j^{3/2}\alpha)} \tag{32}$$

in which J_0 and J_1 are respectively the zero and first-order Bessel functions of the first kind with a complex argument. In the following we will consider the limiting cases of equation (31) for small and large values of the Womersley number.

Small Womersley numbers. To derive the relative impedance I^w for small Womersley numbers, the Bessel functions in equation (32) are approximated by their power series. Following the power series defined in McLachlan [8] the Womersley function can be approximated by

$$F_{10} \simeq \frac{2\frac{j^{3/2}\alpha}{2}[(1 - \frac{\alpha^4}{192}) + j(\frac{\alpha^2}{8} - \frac{\alpha^6}{9216}) + O(\alpha^8)]}{j^{3/2}\alpha[(1 - \frac{\alpha^4}{64}) + j(\frac{\alpha^2}{4} - \frac{\alpha^6}{2304}) + O(\alpha^8)]}. \tag{33}$$

From equation (33) it can be derived that

$$\frac{1}{1-F_{10}} \simeq \frac{(1-\frac{\alpha^4}{64})+j(\frac{\alpha^2}{4}-\frac{\alpha^6}{2304})+O(\alpha^8)}{(-\frac{\alpha^4}{91})+j(\frac{\alpha^2}{8}-\frac{\alpha^6}{3072})+O(\alpha^8)}. \tag{34}$$

Next, for $\alpha^4 \ll 64$ and thus $\alpha \ll 3$, equation (34) can be written approximately as

$$\frac{1}{1-F_{10}} \simeq \frac{1+j\frac{\alpha^2}{4}}{j\frac{\alpha^2}{8}}. \tag{35}$$

Substitution of (35) in (32) then gives the relative impedance I^w,(31), for $\alpha \ll 3$:

$$I^w = 1 + j\frac{\alpha^2}{4}. \tag{36}$$

Large Womersley numbers. For large Womersley numbers the asymptotic expansions for the expressions $J_1(j^{3/2}\alpha)$ and $J_0(j^{3/2}\alpha)$ are used [8]. The Womersley function then reads for $\alpha \gg 1$ [8]:

$$F_{10} \simeq \frac{2}{j^{3/2}\alpha} \frac{\frac{e^{\frac{\alpha}{\sqrt{2}}}}{\sqrt{2\pi\alpha}}[\cos(\frac{\alpha}{\sqrt{2}}-\frac{\pi}{8}+\frac{\pi}{2})+j\sin(\frac{\alpha}{\sqrt{2}}-\frac{\pi}{8}+\frac{\pi}{2})]}{\frac{e^{\frac{\alpha}{\sqrt{2}}}}{\sqrt{2\pi\alpha}}[\cos(\frac{\alpha}{\sqrt{2}}-\frac{\pi}{8})+j\sin(\frac{\alpha}{\sqrt{2}}-\frac{\pi}{8})]}. \tag{37}$$

Because $j^{3/2} = e^{j\frac{3\pi}{4}}$ and $j^{-1/2} = e^{-j\frac{\pi}{4}} = \frac{(1-j)}{\sqrt{2}}$ the expression in (37) can be simplified to

$$F_{10} \simeq \frac{2}{\alpha}e^{-j\frac{\pi}{4}} = \frac{(1-j)\sqrt{2}}{\alpha}. \tag{38}$$

Substituting (38) in (32) gives the relative impedance I^w, (31), for $\alpha \gg 1$:

$$I^w = j\frac{\alpha^2}{8}\frac{1}{1-\frac{(1-j)\sqrt{2}}{\alpha}} = \frac{\alpha^4}{4\sqrt{2}\alpha^3-16\alpha^2+16\sqrt{2}\alpha} + j\frac{\alpha^5-\sqrt{2}\alpha^4}{8\alpha^3-16\sqrt{2}\alpha^2+32\alpha}. \tag{39}$$

Acknowledgments. We would like to thank the Profileringsfonds of the University Hospital Maastricht for the funding of this study.

REFERENCES

[1] D. Bessems, C. G. Giannopapa, M. C. M. Rutten and F. N. van de Vosse, *Experimental validation of a time-domain-based wave propagation model of blood flow in viscoelastic vessels*, J. Biomech., **41** (2008), 284–91.

[2] D. Bessems, M. C. M. Rutten and F. N. van de Vosse, *A wave propagation model of blood flow in large arteries using an approximate velocity profile function*, J. Fluid. Mech., **580** (2007), 145–68.

[3] O. Frank, *Die Grundform des arterielen pulses erste Abhandlung: mathematische analyse*, Z. Biol., **37** (1899), 483–526.

[4] R. Fogliardi, R. Burattini, S. G. Shroff and K. B. Campbell, *Fit to diastolic arterial pressure by third-order lumped model yields unreliable estimates of arterial compliances*, Med. Eng. Phys., **18** (1996), 225–33.

[5] L. R. Hellevik, P. Segers, N. Stergiopulos, F. Irgens, P. Verdonck, C. R. Thompson, K. Lo, R. T. Miyagishima and O. A. Smiseth, *Mechanism of pulmonary venous pressure and flow waves*, Heart Vessels, **14** (1999), 67–71.

[6] G. N. Jager, N. Westerhof and A. Noordergraaf, *Oscillatory flow impedance in electrical analog of arterial system: representation of sleeve effect and non-Newtonian properties of blood* , Circ. Res., **16** (1965), 121–33.

[7] F. Liang and H. Liu, *A closed-loop lumped parameter computational model for human cardiovascular system*, JSME Int. Series C, **48** (2005), 484–93.
[8] N. W. Mc Lachlan, "Bessel Functions for Engineers," Oxford University Press, London, The United Kingdom, 1961.
[9] A. Noordergraaf, P. D. Verdouw and H. B. K. Boom, *The use of an analog computer in a circulation model*, Prog. Cardiovasc. Dis., **5** (1963), 419–439.
[10] M. S. Olufsen and A. Nadim, *On deriving lumped models for blood flow and pressure in the systemic arteries*, Math. Biosc. Eng., **1** (2004), 61–80.
[11] M. S. Olufsen, A. Nadim and A. L. Lewis, *Dynamics of cerebral blood flow regulation explained using a lumped parameter model*, Am. J. Physiol. Regulatory Integrative Comp. Physiol., **282** (2002), R611-R622.
[12] R. Pietrabissa, S. Mantero, T. Marotta and L. Menicanti, *A lumped parameter model to evaluate the fluid dynamics of different coronary bypasses*, Med. Eng. Phys., **18** (1996), 477–84.
[13] P. Segers, N. Stergiopulos, J. J. Schreuder, B. E. Westerhof and N. Westerhof, *Left ventricular wall stress normalization in chronic pressure-overloaded heart: a mathematical model study*, Am. J. Physiol. Heart Circ. Physiol., **279** (2000), H1120–H1127.
[14] N. Stergiopulos, J. J. Meister and N. Westerhof, *Simple and accurate way for estimating total and segmental arterial compliance: the pulse pressure method*, Ann. Biomed. Eng., **22** (1994), 392–97.
[15] N. Stergiopulos, B. E. Westerhof and N. Westerhof, *Total arterial inertance as the fourth element of the windkessel model*, Am. J. Physiol., **276** (2005), H81–88.
[16] N. Westerhof, F. Bosman, C. J. de Vries and A. Noordergraaf, *Analog studies of the human systemic arterial tree*, J. Biomech., **2** (1969), 121–43.
[17] N. Westerhof, G. Elzinga and P. Sipkema, *An artificial arterial system for pumping hearts*, J. Appl. Phys., **31** (1971), 776–81.
[18] J. R. Womersley, *Method for the calculation of velocity, rate of flow and viscous drag in arteries when the pressure gradient is known*, J. Physiol., **127** (1955), 553–63.

Received May 15, 2008; Accepted September 22, 2008.
E-mail address: w.huberts@tue.nl
E-mail address: e.m.h.bosboom@tue.nl
E-mail address: f.n.v.d.vosse@tue.nl